Ultrafast Dynamics and Vibrational Relaxation in Six-Coordinate Heme Proteins Revealed by Femtosecond Stimulated Raman Spectroscopy

Carino Ferrante, Giovanni Batignani, Emanuele Pontecorvo, Linda Montemiglio, Marten H. Vos, Tullio Scopigno

Ultrafast dynamics and vibrational relaxation in six-coordinate heme proteins revealed by Femtosecond Stimulated Raman Spectroscopy.

Carino Ferrante,[†,‡,‖] Giovanni Batignani,[*,†,‖] Emanuele Pontecorvo,[†,‖] Linda C. Montemiglio,[¶] Marten H. Vos,[§] and Tullio Scopigno[*,†,‡]

†*Dipartimento di Fisica, Università di Roma "La Sapienza", I-00185 Rome, Italy*

‡ *Istituto Italiano di Tecnologia, Center for Life Nano Science @Sapienza, Roma, I-00161, Italy*

¶*Dipartimento di Scienze Biochimiche "Alessandro Rossi Fanelli", Università di Roma "La Sapienza", I-00185 Rome, Italy*

§*LOB, Ecole Polytechnique, CNRS, INSERM, Institut Polytechnique de Paris, 91128 Palaiseau Cedex, France*

‖*These authors contributed equally to this work*

E-mail: giovanni.batignani@uniroma1.it; tullio.scopigno@roma1.infn.it

Abstract

Identifying the structural rearrangement and the active sites in photo-induced reactions is a fundamental challenge to understand from a microscopic perspective the underlying dynamics ruling the functional mechanisms of heme proteins. Here, femtosecond stimulated Raman spectroscopy is used to follow the ultrafast evolution of two

six-coordinate heme proteins. By exploiting the sensitivity of Raman spectra to the structural configuration, we investigate the effects of photolysis and binding of amino acid residues in cytochrome c and neuroglobin. Comparing the system response for different time delays and Raman pump resonances, we show how details of atomic motions and energy redistribution can be unveiled.

Introduction

Heme proteins constitute one of the most important families of macromolecular compounds, present in all living organisms and displaying a wide range of biological functions, including oxygen transport and intracellular trafficking. The heme protein's core is an iron atom, confined in a porphyrin ring via four bonds with nitrogen atoms, and able to bind two axial ligands. One of these ligands is usually an amino acid as histidine or methionine. The other ligation site can be occupied by a small gaseous molecule like O_2 or CO, with another amino acid, or be unoccupied. Changes in ligation state are often involved in the function of the heme protein. Therefore, the characterization of the heme-iron bonds and their connection with conformational rearrangements of the porphyrin are crucial for understanding the structural mechanisms ruling the biological role of such prototypical compounds. Notably, several concurring processes, such as structural reconfiguration, energy redistribution and relaxation of intermediate excited states, occur on picosecond and femtosecond timescales, and accompany bond breaking and recombination events. The advent of femtosecond laser sources and the development of optical nonlinear techniques have paved the way to a direct exploration of heme protein ultrafast dynamics.[1–5]

Within such studies, particular efforts have been devoted to the understanding of a rapidly expanding group of proteins, namely those able to form the iron atom sixth bond either with an internal residue or with an external ligand (like O_2, NO or CO). Notably, within this class of proteins, the exchange of internal and external ligands is often thought to be functional. Upon (photo-)dissociation of a gaseous ligands, the kinetics of binding of the

internal residue is rate-limited by migration of the the gaseous ligand through the protein matrix and steric rearrangement,[6–13] whereas dissociation of the heme-residue bond in the absence of external ligands leads to at least 6 orders of magnitude faster rebinding.[14–16]

In particular, the photodissociation and fast rebinding dynamics of the heme-residue bond, occurring on the picosecond time scale (5-9 ps), have been assessed using transient absorption (TA).[17,18] Critically, TA spectroscopy is not able to directly monitor geometrical rearrangements of the heme, neither to distinguish between transient electronic intermediates or de-excitation to a vibrationally hot electronic ground state due to its lack of structural sensitivity.[4,19–21] In contrast, conventional spontaneous Time-Resolved Resonance Raman (TR^3) spectroscopy can provide direct fingerprints of the transient structural configuration of a reacting heme. However, TR^3 temporal and energy resolutions are fundamentally constrained by the Fourier transform limit ($\Delta E \Delta t \geq 15\,\mathrm{cm}^{-1}\mathrm{ps}$), making it difficult to resolve spectral details arising from ultrafast dynamics on the $\lesssim$ 1ps timescale.

Nevertheless, using an accurate balance of the two resolutions, Cianetti et al. provided useful insight on the photolysis observing the appearance, in ferrous six-coordinate (6-c) cytochrome *c* (cyt *c*), of a low frequency Raman band (centered at 216 cm^{-1} and assigned to the iron-histidine stretching mode) sensitive to the doming of the porphyrin ring at the picosecond time scale.[22]

In this work, in order to circumvent the TR^3 limitations, we take advantage of the recently introduced Femtosecond Stimulated Raman Spectroscopy (FSRS) non-linear technique,[23–25] combining both high spectral and temporal resolutions.[26–29] The experimental scheme requires three pulses, a femtosecond actinic pump (AP), that triggers the dynamic of interest, a Raman pulse (RP) and a broadband probe pulse (PP), to probe photoreactions with uncompromised temporal precision (down to 50 fs) and spectral resolution (a few wavenumbers) via stimulated Raman scattering.[24] Specifically, probing transient stimulated vibrational spectra and taking advantage of the wavelength tunability of a narrowband Raman pulse,[30,31] FSRS has proven able to assign contributions arising from different intermediate states and

to provide important insights on femtosecond structural changes upon photo-excitation.[32–36] By comparing the Raman band cross sections and positions, measured scanning the RP wavelength across the absorption bands of transient and relaxed species,[37,38] it is possible to extract detailed structural information on the system dynamics: for this reason we developed a FSRS setup with a tunable Raman pulse (Femtosecond Stimulated Resonance Raman Scattering, FSRRS) able to explore resonance effects across all the Soret absorption band (400-460 nm).[39] Here we study two heme proteins with the hemes in the ferrous 6-c form with two amino acid ligands: cyt *c* and neuroglobin (Ngb). Ngb is a relatively recently discovered protein,[40] which is present predominantly in brain and nerve tissues and whose biological function is still elusive. As the prototypical oxygen-storage protein myoglobin (Mb) it can easily bind small gaseous ligands to the *b*-type heme cofactor, but whereas the heme in unliganded deoxy-myoglobin is 5-c in the absence of external ligands in Ngb it is 6-c with two histidine residus as ligands. cyt *c* is an ubiquitous and well-studied soluble electron transfer heme protein. During its electron transfer function it switches between the ferric and ferrous state, always remaining 6-c with histidine and methionine as axial ligands. Other than globin heme proteins it does not readily bind external ligands, except when it is modified by interactions with lipids.[41,42] It is also relatively rigid,[43,44] a property thought favorable for its electron transfer function.[45] Another important difference with Ngb is that it carries a *c*-type heme, which implies that the heme binds to the protein not only via the iron atom but also via two covalent bonds of the peripheral vinyl groups with cysteine residues.[46] The external ligand[47] and one of the internal ligands in ferrous 6-c heme proteins not binding external ligands[18] can be photo-dissociated with high quantum yield. Our Raman results elucidate the detail of the dynamics upon the photo-excitation, allowing to discern between structural modification and energy transfer in such molecules. Specifically we find a new marker of internal ligand photolysis in the high frequency region (ν_4 at 1360 cm^{-1}) common for both the molecules and molecule-specific cooling processes that involve different Raman modes.

Results

To visualize the electronical resonances of the system, TA spectra of photo-excited ferrous Mb (5-c), cyt c and Ngb are reported in Fig. 1, with a sketch of the heme pockets for the three different protein species reported in the right panel. Notably, in view of the absence of the axial distal ligand, the photo-dynamics of the 5-c heme in Mb is in principle distinguished from 6-c hemes due to the absence of photolysis and is characterized only by an energy transfer for times > 50 fs.[20,38] Although the structural pathway is different, the TA spectra measured in the Soret band are qualitatively similar, characterized by a dispersive shape with a maximum absorption red-shifted with respect to the Soret band, testifying the poor structural sensitivity of TA.

More quantitatively, in Fig. 1a-b-c, after the instantaneous appearance of a dispersive feature in TA data, the recovery of the initial absorption profile occurs faster in the Mb case (≈ 3 ps) than for the two 6-c hemes (≈ 8 ps for Ngb and ≈ 5 ps for cyt c) (cf. refs.[18,21]).

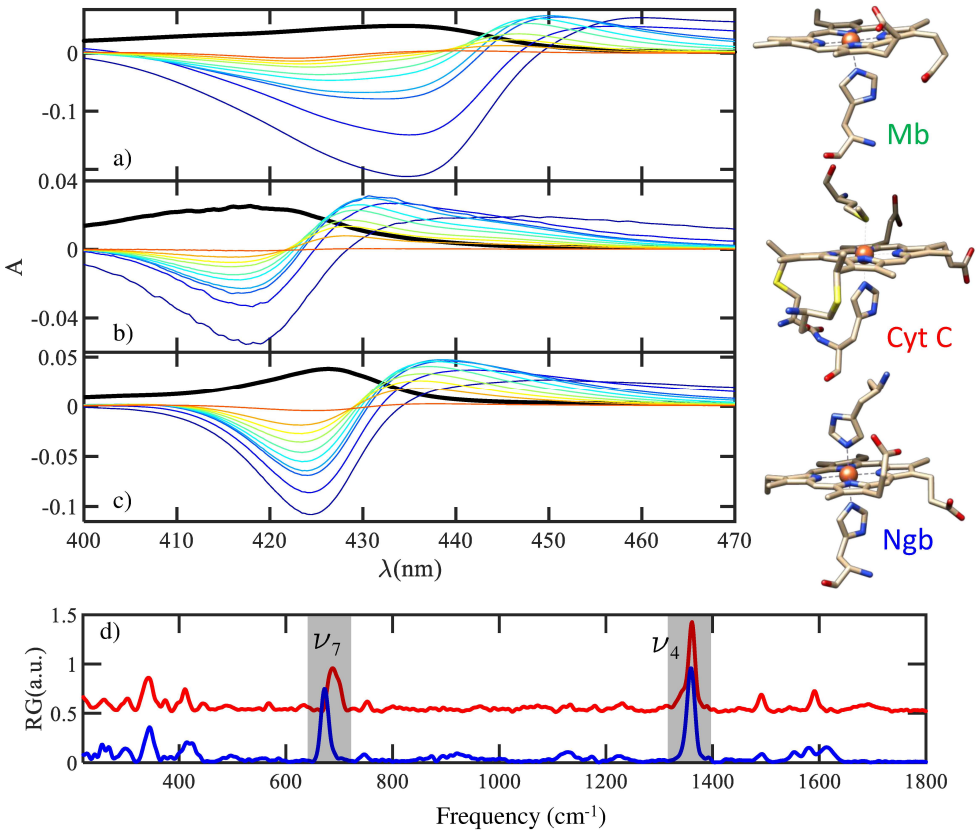

Figure 1: TA traces around the Soret band for different time delays in Mb (a), cyt c (b) and Ngb (c) are reported as colored lines in panels a-b-c. The time delays are 0.1, 0.3, 0.5, 1, 2, 3, 5 ,7, 10, 30 ps from blue to red. The scaled static absorption profiles are reported as black lines. In d) we report the cyt c and Ngb static stimulated Raman spectra, measured with a RP tuned at 430 nm (red and blue lines, respectively). The two main peaks at ~ 700 and ~ 1350 cm^{-1} are the ν_7 and ν_4 respectively.

A careful inspection of the TA spectra also reveals the presence of a sub-picosecond more red-shifted tail, possibly related to the heating effects. Such relaxation is present for all the three investigated species[16,18,48] and it occurs on a femtosecond timescale (from ≈ 150 fs in cyt c to ≈ 400 fs in Ngb and Mb).

Steady-state stimulated Raman spectra of cyt c and Ngb, measured tuning the RP in resonance with the Soret band absorption setup without AP, are also reported in fig. 1d and reveals two dominant modes (ν_7 and ν_4), corresponding to totally symmetric in-plane breathing modes of the porphyrin ring.

Cytochrome c

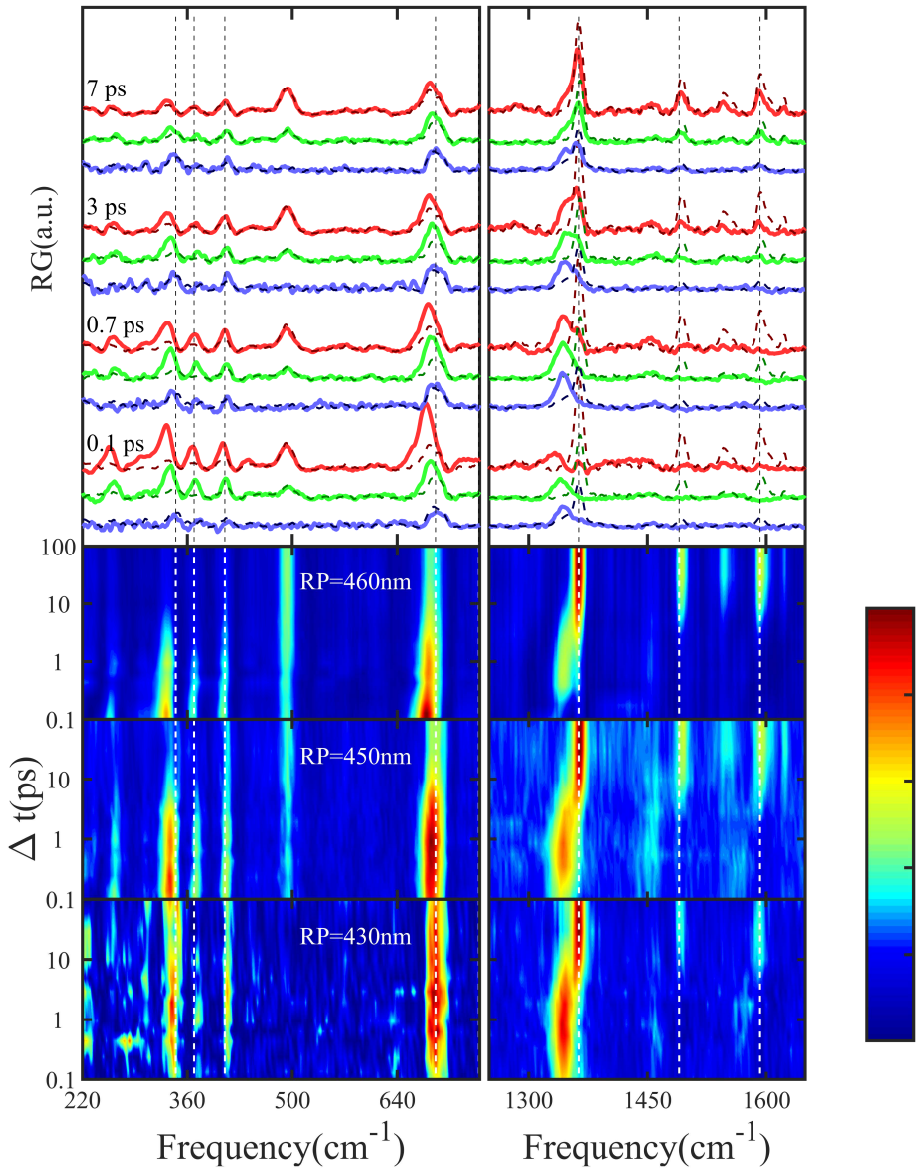

Figure 2: FSRRS spectra of ferrous cyt *c* (solid lines) are shown for selected time delays with the RP at 460 nm (red), 450 nm (green) and 430 (blue). Reference spectra in the absence of the AP are also reported as dashed lines. b, The corresponding FSRRS colour maps are reported for all the measured time delays from 0.1 to 100 ps. The vertical dashed lines are guides to the eye. The unphotoexcited contribution has been removed and probe chirp temporal shifts have been corrected.

The FSRRS measurements of cyt c offer a direct way to follow the molecular dynamics. The experimental data, reported in Fig. 2, show two main features: (i) a shift of ν_4 position from 1360 cm^{-1} to $\sim$ 1342 cm^{-1} on the time scale of a few picoseconds and (ii) a shift to lower energy of the vibrational mode up to 700 cm^{-1} more pronounced for higher RP wavelengths. The latter effect, more evident during the first 1 ps, can be attributed to an out-of-equilibrium heating of vibrational modes,[17] corresponding to an increase of the population of vibrationally excited states. This implies the appearance in the Raman spectrum of hot bands, i.e. Raman transition from vibrationally excited levels ($n > 0$) to the higher ones ($n+1$) . Hot bands are generally centered at lower wave-numbers with respect to the fundamental bands ($0 \rightarrow 1$), due to anharmonic molecular potentials (a further discussion is reported in the SI), and are more visible for RP wavelengths which are red-shifted with respect to Soret band maximum.[38] On the contrary, the 1342 cm^{-1} ν_4 band cannot be ascribed to a hot band of the "fundamental" contribution (at $\sim$ 1360 cm^{-1}) because it does not undergo an amplitude enhancement for red-shifted RP wavelengths at any of the monitored time delays, and because the picosecond ($\sim$ 1360 cm^{-1}) band is weaker than the shifted peak also in resonance with the vibrational ground state (at RP=430 nm), incompatible with a thermal distribution of vibrational levels, where the population of the n=1 level can not be larger than that of the n=0 level. Moreover, the shifted peak, reported as a red dashed line in Fig.3, shows a frequency dynamics compatible with the evolution in an out-of-equilibrium configuration (see below) and not with hot band population, which would show a time-independent energy difference between the vibrational levels.

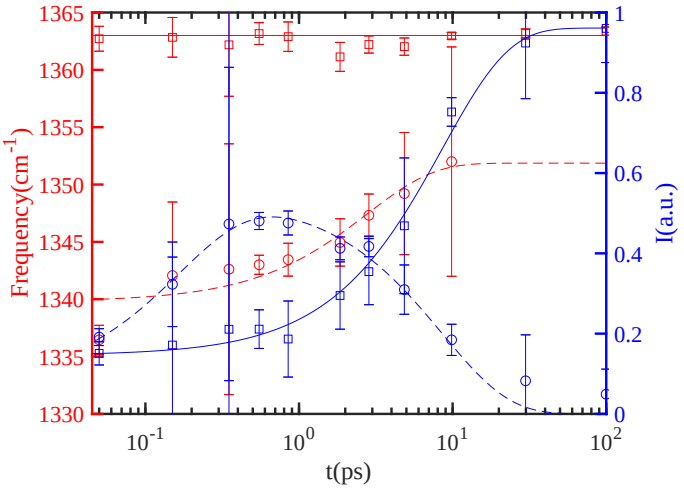

Figure 3: The intensity (blue axis) and frequency (red axis) of ν_4^{gs} (squares) and ν_4^{pd} (circles) are reported for different time delays, extracted from the measurements with the RP tuned at 450 nm. Time dependent amplitudes and positions are extracted fitting the experimental spectra with Gaussian profiles. The ν_4^{pd} position is not reported for time delays with vanishing ν_4^{pd} intensity. The recovery of the ν_4^{gs} peak amplitude is simultaneous with the disappearance of ν_4^{pd}, which shows a frequency shift (red dashed line) of $\sim$ 10 cm^{-1}. The kinetics of the relaxation process are obtained by mono and bi-exponential fits of peak amplitudes and positions (reported as lines). Specifically, the characteristic times are for ν_4^{pd} intensity 0.18 and 8.6 ps, for ν_4^{gs} intensity 8.6 ps and for ν_4^{pd} peak position 2.8 ps.

Considering the recombination time scale of the residue binding,[17,18,49] the spectrally resolved transient 1340-1350 cm^{-1} ν_4 peak can be assigned to the methionine-photodissociated 5-c heme. Consequently, hereafter we refer to the two contributions as ground state and photodissociated state (ν_4^{gs} and ν_4^{pd}, respectively).

Interestingly, the same measurement was performed also with TR^3,[16] where the upshift of the ν_4 band on the picosecond timescale was assigned to vibrational cooling related to anharmonic coupling of the ν_4 band to lower-frequency bands. This view is in agreement with the evolution of the ν_7 mode described here and discussed above. We note that the time constant of the shift was found to be somewhat shorter in the present FSRS work (2.8 ps) than in the TR3 experiments (6.8 ps). This difference is presumably related to the much lower TR3 spectral resolution, which leads to uncertainty in distinguishing the two ν_4 contributions.

Neuroglobin

The FSRRS spectra of photoexcited ferrous Ngb, measured with a RP tuned at 460 nm, are reported in Fig. 4 and show at first sight similar trends as those recorded for the cyt c case. Evident are the downshift of the of vibrational modes up to 700 cm^{-1} on the picosecond timescale due to heating and the intense shifted ν_4 component occurring within the first 10 ps. Interestingly, the transient ν_4 spectral component has a shape with a distinctly asymmetric red-tail (see the solid line at 0.7 ps of Fig. 4).

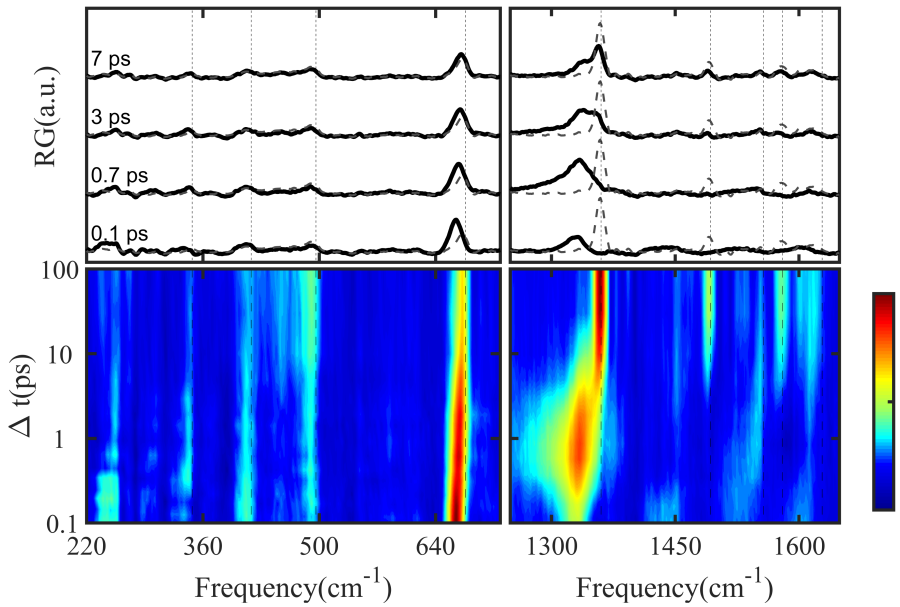

Figure 4: FSRRS spectra of ferrous Ngb (solid lines) are shown for selected time delays. Reference spectra in the absence of the actinic pulse are reported as dashed lines. b, The corresponding FSRRS colour maps are reported for all the measured time delays from 0.1 to 100 ps. The vertical dashed lines are guides to the eye. The RP wavelength is set at 460 nm, the unphotoexcited contribution has been removed and probe chirp temporal shifts have been corrected.

To understand the origin of this contribution we compare the same measurement at 1 ps of time-delay (in which the contribution of ν_4^{gs} is negligible) for different RP wavelengths in the red side of Soret band, as shown in Fig.5. The results demonstrate the large dependence of the red tail on the RP wavelength, as expected for the scenario of hot bands.[38] Moreover,

the broad bandwidth of such contribution ($\sim 50\text{cm}^{-1}$, highlighted by the red area in Fig.5) indicates a lifetime of the first vibrationally excited state much shorter than that of the ground state.

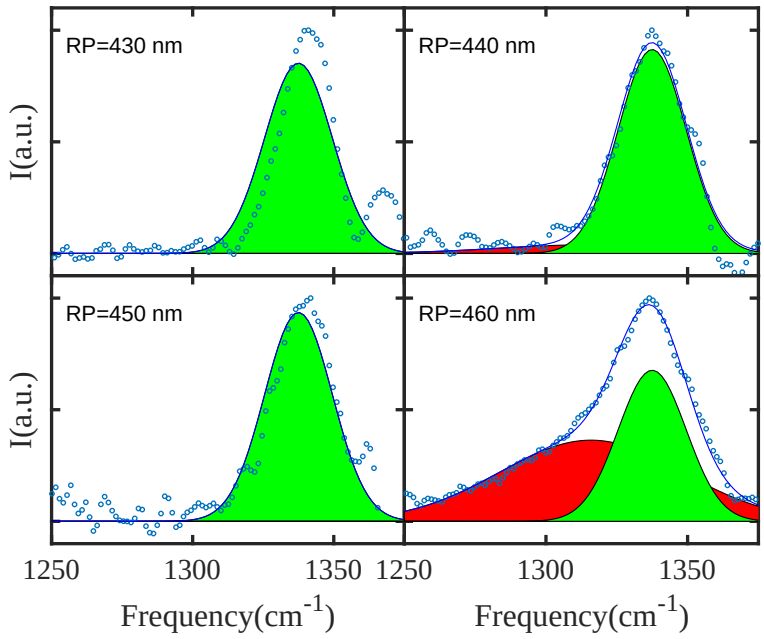

Figure 5: FSRRS ν_4 spectra of ferrous Ngb (blue circles), after subtraction of the non-excited molecular fraction, at 1 ps and different RP wavelength. For this time delay the experimental data can be fitted (blue line) with two gaussians, that represent ν_4^{pd} (green area) and hot band of ν_4^{pd} (red area). The contribution of ν_4^{gs} is negligible for this time-delay. In agreement with Ref.,[38] the hot-band contribution is emphasized with RP red-shift.

Moreover, the peak positions of ν_4^{pd} and hot band of ν_4^{pd}, reported in fig. 6, have a similar trend and, consequently, a constant difference of $\sim$ 25 cm^{-1}. This implies that during the structural evolution in the photo-dissociated state the anharmonicity factor is almost constant. Assuming a Morse potential, the anharmonicity factor α is ~ 0.0088 (see SI), 2 times greater than the value extracted for Myoglobin ($\alpha = 0.004$).[38]

Summing up, Ngb shows also a Raman signature of the photodissociated state, in this case for the photolysis of histidine (ref.[18]), with a transient hot ν_4 vibrational state which decays on the picosecond time scale , analogously to the case of excited deoxy Mb[38] (see SI). The latter feature represents an important difference with respect to cyt c, that does not show this heating of the ν_4 vibrational mode.

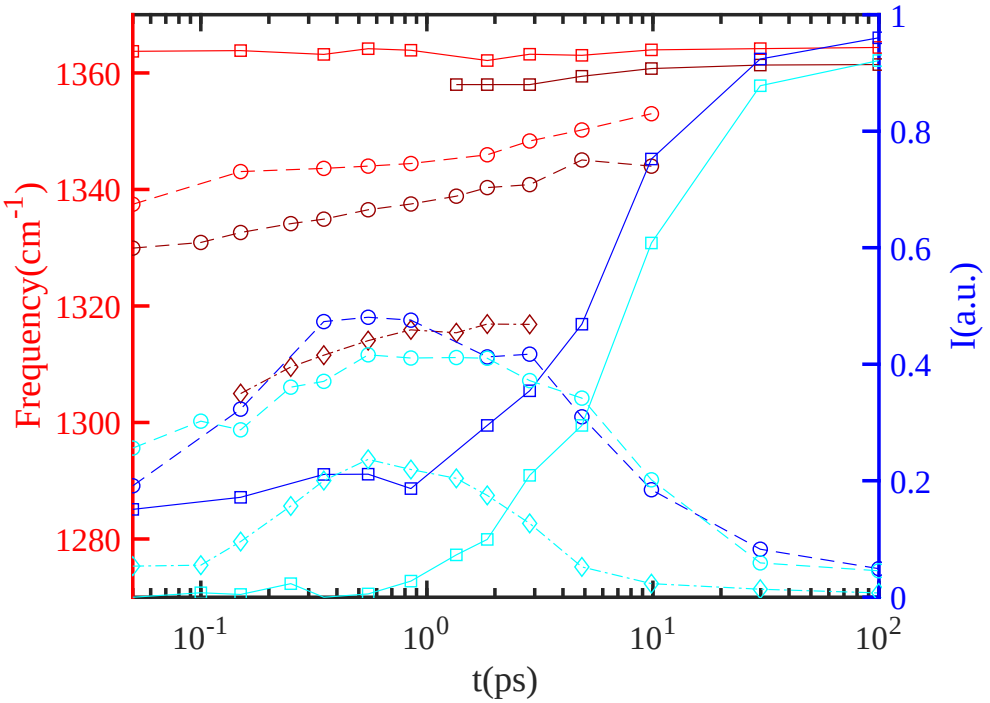

Figure 6: The intensity of cyt c (blue lines) and Ngb (cyan lines) and frequency of cyt c (red lines) and Ngb (brown lines) of ν_4^{gs} (squares), ν_4^{pd} (circles) and hot bands of ν_4^{pd} (diamonds) are reported for different time delays. Time dependent amplitudes and positions are extracted fitting the experimental spectra with Gaussian profiles. The peak position is reported only for intensity $I(t)$ larger than $0.08I(-10\text{ps})$. The recovery of ν_4^{gs} intensity is simultaneous with the disappearance of ν_4^{pd}, that has a frequency shift (red dashed line) of ~ 10 cm^{-1}.

Discussion

In the literature photolysis of amino acid residues (i.e. histidine, methionine, etc..) from ferrous hemes has been mainly investigated by TA spectroscopy.[18] The only Raman evidence of bond breaking obtained by ps-time-resolution spontaneous TR^3 is the appearance in cyt c of the iron-histidine band,[22] following vibrational coherence spectroscopy assignments.[17] Vibrational cooling following photolysis on the picosecond time scale has been studied by TR^3, but here the poor spectral and temporal resolution limits the obtainable information on the evolution of the dissociated configuration and in particular does not allow to resolve hot bands. FSRRS transient spectra allow to exploit the marker of photolysis in the region

of ν_4. Moreover, FSRRSâĂŹ high spectral and temporal resolutions enabled us to disclose marked differences in the structural dynamics and energy flow in the investigated b- and c-type hemes. The results are summarized in fig. 7.

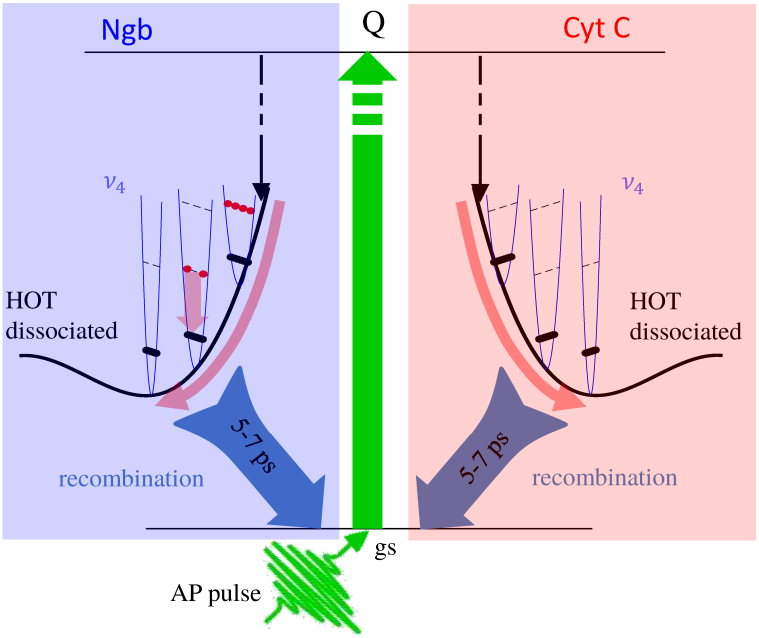

Figure 7: The interaction with the AP pulse promotes the system from the ground state to the Q band in both 6-c molecules. The system decays instantaneously ($<$ 50 fs) into the hot photodissociated state of Ngb (blue area) and cyt c (red area), in which the internal residue (histidine for Ngb and methionine for cyt c) is detached from the iron atom. In this condition a cooling process and a structural relaxation can be observed. The observation of hot band of ν_4^{pd} testifies the population of vibrational excited in Ngb (red circles in ν_4 potential). The last step is the recovery of the ground state in 5-9 ps with the binding of the residue.

Structural dynamics

In two 6-c molecules examined, the frequency position of ν_4^{gs} is very similar and also the dynamics of the ν_4^{pd} are practically equivalent, as quantified by red and brown dashed lines in fig. 6. Particularly, after an instantaneous softening of ν_4^{pd} mode, a partial recovery toward the gs frequency is observed before the full relaxation to the 6-c ground state. This recovery, quantified in fig. 3, can be interpreted in two different ways: anharmonic mode coupling with a low frequency mode[4] or a picosecond geometrical reorganization able to accommodate

the recombination of the distal ligand after its instantaneous photolysis.[36] Notably, the observation of the ν_4^{pd} hot band only for the Ngb case suggests a ν_4 coupling different for the two 6-c systems,[38] which would imply different trends (which was not observed) if the ν_4^{pd} peak shifts were due to anharmonic coupling. Moreover, in striking contrast with the ν_4^{pd} dynamics measured in Mb, where the anharmonic coupling induces an initial ≈ 4 cm^{-1} peak red-shift followed by a recovery,[38] the ν_4^{pd} peak measured in both the 6-c molecules shows a strong (> 10 cm^{-1}) and monotonic (in time) blue-shift (see fig. S2 of the SI). Taken together, these results point to the presence of a picosecond geometrical reorganization. Therefore, we can deduce that the picosecond geometrical reorganization sensed by the ν_4 vibrational coordinate is a general feature in the process of bond breaking/reformation of ferrous heme with an internal residue.

Energy flow

The hot bands dynamics, observed in the two 6-c systems, show an out-of-equilibrium energy distribution in the photo-dissociated intermediate state, with a key role of the vibrational modes up to 700 cm^{-1}, as in the case of 5-c Mb.[38] Specifically, these hot bands are the signature of a high temperature distribution of vibrational excited states and appear in less than 100 fs, testifying the crucial role of these modes as thermal receptors. Moreover the picosecond recovery of the cold state highlights their efficiency in the flowing of thermal energy out of the heme via coupling to low-frequency (delocalized) modes of the protein environment. The scenario is quite different for high frequency modes and, specifically, for the ν_4 band. In the case of 5-c Mb a picosecond trapping of thermal energy in the n=1 level of the ν_4 mode is observed. Starting from 6-c heme systems a 5-c hot heme state is also populated, albeit with less vibrational energy due to the energy required for dissociating the Fe-residue bond (which is yet only a small fraction of the energy of the absorbed photon, at least for cyt c[50]) and the dynamics is complicated by the photolysis process. The photo-dissociated Ngb shows a very prominent ν_4 hot band effect very similar

to the Mb case. However, in cyt c no population of higher ν_4 vibrational levels is observed on the same timescale. This finding implies that either these levels don't get significantly populated from the initial broad manifold of vibrational states (ref.[38])) or that they very rapidly (< 100fs) decay to the n=0 level. Notably, this interpretation implies a most efficient cooling process in cyt c, that can explain the shorter time scale of red-tail in TA (150 fs). We assign this striking difference between cyt c and Ngb to the fact that the c-type heme is not only bound axially to the protein via the heme iron but also via two covalent bonds with cysteine residues at the periphery of the heme plane. Therefore the effective coupling of the ν_4 in-plane mode to protein modes in the same frequency range will be much stronger and energy redistribution with high-frequency protein modes more efficient. Energy flow has been modelled in a number of heme proteins and several studies have been devoted to cyt c.[43,51–54] In comparison with similar studies on myoglobin[52] it was indeed observed that through-bond energy flow plays a much stronger role in cyt c in particular by flow through the cross-linked cysteine residues, including on the 100-fs timescale.[55] In a different study, the cysteines were found to respond with a rate > 500 ps^{-1} even when the excess energy was deposited initially only in the close vicinity of the heme iron.[54] These studies thus appear in qualitative agreement with the present experimental work. Mode-resolved theoretical analyses may allow a more detailed comparison with the FSRS data.

Experimental section

Sample preparation

The murine deoxy Neuroglobin is prepared dissolving the freeze-dried ferric form[56] in a phosphate buffer, pH 7.4, and the obtained solution is purified into a biochemical basket centrifuge. Sodium dithionite ($Na_2S_2O_4$) is used to reduce the ferric Neuroglobin to ferrous form. The reduction of the protein was done in a nitrogen-purged buffer to avoid exposure to atmospheric oxygen. The concentrations of the samples are between 100 and 200 μM.

Horse-heart cyt c was purchased from Sigma and prepared as described above for Neuroglobin.

The sample is allowed to flow anaerobically through the transmission cell during the experiment due to a peristaltic pump, so as to guarantee a fresh sample at every laser shot (1 KHz). All Raman measurements were performed at room temperature. The transmission cell is mounted onto an upright motorized translator, to allow regular movements to minimize window damaging by the three beams.

FSRS setup

A detailed description of our FSRRS setup has been given elsewhere.[30,39,57] The basic concept is to use a $\sim$1 μJ-energy, 50 fs-time-duration AP tuned in the heme Q-band (550 nm) to photo-excite the system, triggering the dynamics of interest. The system evolution is then monitored by a couple of a narrowband tunable Raman pulse (RP), which provides the spectral resolution, and a broadband femtosecond probe pulse (PP), which guarantees the time precision. The joint action of temporally and spatially overlapped RP and PP allows to record Stimulated Raman scattering (SRS) spectra, coherently generated on top of the highly directional PP and hence essentially free from fluorescence background. The TA measurements, recorded in absence of the RP, have been performed with the same pulse properties.

Conclusions

In conclusion, the observation of Raman evolution in 6-c heme proteins with high spectral and temporal resolution allows to discriminate a new marker of photolysis related to a red shifted contribution of ν_4 Raman mode. In addition, the dynamics of hot band contribution unveils the pathway of thermal relaxation in such macromolecules. In particular, we detected an high out equilibrium condition in the photolysed state, consisting in a high temperature of

low vibrational modes (up to 700 cm^{-1}). Interestingly in Ngb a trapping of thermal energy in the n=1 level is observed for the vibrational coordinate of ν_4, but not in cyt *c*. This finding presumably finds its structural origin in the different heme-protein-bonding in these proteins and may be related to the difference in rigidity required for the respectively small molecule- and electron-transfer functions of these proteins. After the recombination of the internal ligand, the systems are fully relaxed in the gs, without any residual thermal heating effect.

Acknowledgement

The authors thank B. Vallone and the Dipartimento di Scienze Biochimiche and Istituto Pasteur-Fondazione Cenci Bolognetti of Università di Roma "La Sapienza" for the support with sample preparation. We acknowledge M. Brunori for many inspiring discussions.

Supporting Information Available

The following files are available free of charge.

- SupplementaryMaterial.pdf: supporting information with (i) anharmonicity factor extracted from the FSRRS spectra and (ii) comparison between five-coordinate (Mb) and six-coordinate (Ngb and cyt *c*) ν_4 peak dynamics.

References

(1) Mizutani, Y.; Kitagawa, T. Direct Observation of Cooling of Heme Upon Photodissociation of Carbonmonoxy Myoglobin. *Science* **1997**, *278*, 443–446.

(2) Rosca, F.; Kumar, A. T. N.; Ionascu, D.; Sjodin, T.; Demidov, A. A.; Champion, P. M.

Wavelength selective modulation in femtosecond pump–probe spectroscopy and its application to heme proteins. *J. Chem. Phys* **2001**, *114*, 10884.

(3) Kholodenko, Y.; Volk, M.; Gooding, E.; Hochstrasser, R. Energy dissipation and relaxation processes in deoxy myoglobin after photoexcitation in the Soret region. *Chemical Physics* **2000**, *259*, 71–87.

(4) Franzen, S.; Kiger, L.; Poyart, C.; Martin, J.-L. Heme Photolysis Occurs by Ultrafast Excited State Metal-to-Ring Charge Transfer. *Biophysical Journal* **2001**, *80*, 2372–2385.

(5) Vos, M. H. Ultrafast dynamics of ligands within heme proteins. *Biochimica et Biophysica Acta (BBA) - Bioenergetics* **2008**, *1777*, 15 – 31.

(6) Kruglik, S. G.; Yoo, B.-K.; Lambry, J.-C.; Martin, J.-L.; Negrerie, M. Structural changes and picosecond to second dynamics of cytochrome c in interaction with nitric oxide in ferrous and ferric redox states. *Physical Chemistry Chemical Physics* **2017**, *19*, 21317–21334.

(7) Vos, M. H.; Liebl, U. Time-resolved infrared spectroscopic studies of ligand dynamics in the active site from cytochrome c oxidase. *Biochimica et Biophysica Acta (BBA) - Bioenergetics* **2015**, *1847*, 79–85.

(8) Hargrove, M. S. A Flash Photolysis Method to Characterize Hexacoordinate Hemoglobin Kinetics. *Biophysical Journal* **2000**, *79*, 2733–2738.

(9) Hvitved, A. N.; Trent, J. T.; Premer, S. A.; Hargrove, M. S. Ligand Binding and Hexacoordination in SynechocystisHemoglobin. **2001**, *276*, 34714–34721.

(10) Kriegl, J. M.; Bhattacharyya, A. J.; Nienhaus, K.; Deng, P.; Minkow, O.; Nienhaus, G. U. Ligand binding and protein dynamics in neuroglobin. **2002**, *99*, 7992–7997.

(11) Trent, J. T.; Watts, R. A.; Hargrove, M. S. Human Neuroglobin, a Hexacoordinate Hemoglobin That Reversibly Binds Oxygen. **2001**, *276*, 30106–30110.

(12) Puranik, M.; Nielsen, S. B.; Youn, H.; Hvitved, A. N.; Bourassa, J. L.; Case, M. A.; Tengroth, C.; Balakrishnan, G.; Thorsteinsson, M. V.; Groves, J. T.; McLendon, G. L.; Roberts, G. P.; Olson, J. S.; Spiro, T. G. Dynamics of Carbon Monoxide Binding to CooA. **2004**, *279*, 21096–21108.

(13) Gonzalez, G.; Dioum, E. M.; Bertolucci, C. M.; Tomita, T.; Ikeda-Saito, M.; Cheesman, M. R.; Watmough, N. J.; Gilles-Gonzalez, M.-A. Nature of the Displaceable Heme-Axial Residue in the EcDos Protein, a Heme-Based Sensor from Escherichia coli. *Biochemistry* **2002**, *41*, 8414–8421.

(14) Jongeward, K. A.; Magde, D.; Taube, D. J.; Traylor, T. G. Picosecond kinetics of cytochromes b5 and c. **1988**, *263*, 6027–6030.

(15) Kumazaki, S.; Nakajima, H.; Sakaguchi, T.; Nakagawa, E.; Shinohara, H.; Yoshihara, K.; Aono, S. Dissociation and Recombination between Ligands and Heme in a CO-sensing Transcriptional Activator CooA: A FLASH PHOTOLYSIS STUDY. **2000**, *275*, 38378–38383.

(16) Negrerie, M.; Cianetti, S.; Vos, M. H.; Martin, J.-L.; Kruglik, S. G. Ultrafast Heme Dynamics in Ferrous versus Ferric Cytochrome c Studied by Time-Resolved Resonance Raman and Transient Absorption Spectroscopy. *The Journal of Physical Chemistry B* **2006**, *110*, 12766–12781.

(17) Wang, W.; Ye, X.; Demidov, A. A.; Rosca, F.; Sjodin, T.; Cao, W.; Sheeran, M.; Champion, P. M. Femtosecond Multicolor Pump-Probe Spectroscopy of Ferrous Cytochromec†. *The Journal of Physical Chemistry B* **2000**, *104*, 10789–10801.

(18) Vos, M. H.; Battistoni, A.; Lechauve, C.; Marden, M. C.; Kiger, L.; Desbois, A.; Pilet, E.; de Rosny, E.; Liebl, U. Ultrafast Heme-Residue Bond Formation in Six-

Coordinate Heme Proteins: Implications for Functional Ligand Exchange. *Biochemistry* **2008**, *47*, 5718–5723.

(19) Lim, M.; Jackson, T. A.; Anfinrud, P. A. Femtosecond Near-IR Absorbance Study of Photoexcited Myoglobin: Dynamics of Electronic and Thermal Relaxation. *The Journal of Physical Chemistry* **1996**, *100*, 12043–12051.

(20) Ye, X.; Demidov, A.; Rosca, F.; Wang, W.; Kumar, A.; Ionascu, D.; Zhu, L.; Barrick, D.; Wharton, D.; Champion, P. M. Investigations of Heme Protein Absorption Line Shapes, Vibrational Relaxation, and Resonance Raman Scattering on Ultrafast Time ScalesâĂă. *The Journal of Physical Chemistry A* **2003**, *107*, 8156–8165.

(21) Petrich, J. W.; Poyart, C.; Martin, J.-L. Photophysics and reactivity of heme proteins: a femtosecond absorption study of hemoglobin, myoglobin, and protoheme. *Biochemistry* **1988**, *27*, 4049–4060.

(22) Cianetti, S.; Négrerie, M.; Vos, M. H.; Martin, J.-L.; Kruglik, S. G. Photodissociation of Heme Distal Methionine in Ferrous Cytochrome c Revealed by Subpicosecond Time-Resolved Resonance Raman Spectroscopy. *Journal of the American Chemical Society* **2004**, *126*, 13932–13933.

(23) Yoshizawa, M.; Hattori, Y.; Kobayashi, T. Femtosecond time-resolved resonance Raman gain spectroscopy in polydiacetylene. *Phys. Rev. B* **1994**, *49*, 13259–13262.

(24) Kukura, P.; McCamant, D. W.; Mathies, R. A. Femtosecond Stimulated Raman Spectroscopy. *Annu. Rev. Phys. Chem.* **2007**, *58*, 461–488.

(25) McCamant, D. W.; Kukura, P.; Yoon, S.; Mathies, R. A. Femtosecond broadband stimulated Raman spectroscopy: Apparatus and methods. *Rev. Sci. Instrum.* **2004**, *75*, 4971–4980.

(26) Mukamel, S.; Biggs, J. D. Communication: Comment on the effective temporal and spectral resolution of impulsive stimulated Raman signals. *J. Chem. Phys.* **2011**, *134*, 161101.

(27) D. W. McCamant, Re-Evaluation of Rhodopsin's Relaxation Kinetics Determined from Femtosecond Stimulated Raman Lineshapes. *J. Phys. Chem. B* **2011**, *115*, 9299–9305.

(28) Fumero, G.; Batignani, G.; Dorfman, K. E.; Mukamel, S.; Scopigno, T. On the Resolution Limit of Femtosecond Stimulated Raman Spectroscopy: Modelling Fifth-Order Signals with Overlapping Pulses. *ChemPhysChem* **2015**, *16*, 3438–3443.

(29) Batignani, G.; Fumero, G.; Pontecorvo, E.; Ferrante, C.; Mukamel, S.; Scopigno, T. Genuine dynamics vs cross phase modulation artefacts in Femtosecond Stimulated Raman Spectroscopy. *ACS Photonics* **2019**, *6*, 492–500.

(30) Pontecorvo, E.; Kapetanaki, S.; Badioli, M.; Brida, D.; Marangoni, M.; Cerullo, G.; Scopigno, T. Femtosecond stimulated Raman spectrometer in the 320-520nm range. *Opt. Express* **2011**, *19*, 1107–1112.

(31) D. P. Hoffman, D. Valley, S. R. Ellis, M. Creelman, R. A. Mathies, Optimally shaped narrowband picosecond pulses for femtosecond stimulated Raman spectroscopy. *Opt. Express* **2013**, *21*, 21685.

(32) Fang, C.; Frontiera, R. R.; Tran, R.; Mathies, R. A. Mapping GFP structure evolution during proton transfer with femtosecond Raman spectroscopy. *Nature* **2009**, *462*, 200–204.

(33) Kuramochi, H.; Takeuchi, S.; Tahara, T. Ultrafast Structural Evolution of Photoactive Yellow Protein Chromophore Revealed by Ultraviolet Resonance Femtosecond Stimulated Raman Spectroscopy. *J. Phys. Chem. Lett.* **2012**, *3*, 2025–2029.

(34) A. L. Dobryakov, I. Ioffe, A. A. Granovsky, N. P. Ernsting, S. A. Kovalenko, Femtosecond Raman spectra of cis-stilbene and trans-stilbene with isotopomers in solution. *J. Chem. Phys.* **2012**, *137*, 244505.

(35) Batignani, G.; Bossini, D.; Palo, N. D.; Ferrante, C.; Pontecorvo, E.; Cerullo, G.; Kimel, A.; Scopigno, T. Probing ultrafast photo-induced dynamics of the exchange energy in a Heisenberg antiferromagnet. *Nature Photon.* **2015**, 506–510.

(36) Batignani, G.; Pontecorvo, E.; Ferrante, C.; Aschi, M.; Elles, C. G.; Scopigno, T. Visualizing Excited-State Dynamics of a Diaryl Thiophene: Femtosecond Stimulated Raman Scattering as a Probe of Conjugated Molecules. *J. Phys. Chem. Lett.* **2016**, *7*, 2981–2988.

(37) Batignani, G.; Pontecorvo, E.; Giovannetti, G.; Ferrante, C.; Fumero, G.; Scopigno, T. Electronic resonances in broadband stimulated Raman spectroscopy. *Sci. Rep.* **2016**, *6*, srep18445.

(38) Ferrante, C.; Pontecorvo, E.; Cerullo, G.; Vos, M. H.; Scopigno, T. Direct observation of subpicosecond vibrational dynamics in photoexcited myoglobin. *Nat. Chem.* **2016**, *8*, 1137–1143.

(39) Pontecorvo, E.; Ferrante, C.; Elles, C. G.; Scopigno, T. Spectrally tailored narrowband pulses for femtosecond stimulated Raman spectroscopy in the range 330-750 nm. *Opt. Express* **2013**, *21*, 6866–6872.

(40) Burmester, T.; Weich, B.; Reinhardt, S.; Hankeln, T. A vertebrate globin expressed in the brain. *Nature* **2000**, *407*, 520–523.

(41) Schonhoff, C. M.; Gaston, B.; Mannick, J. B. Nitrosylation of Cytochrome c during Apoptosis. *Journal of Biological Chemistry* **2003**, *278*, 18265–18270.

(42) Kapetanaki, S. M.; Silkstone, G.; Husu, I.; Liebl, U.; Wilson, M. T.; Vos, M. H. Interaction of Carbon Monoxide with the Apoptosis-Inducing Cytochromec-Cardiolipin Complex†. *Biochemistry* **2009**, *48*, 1613–1619.

(43) Wong, C. F.; Zheng, C.; Shen, J.; McCammon, J. A.; Wolynes, P. G. Cytochrome c: a molecular proving ground for computer simulations. *The Journal of Physical Chemistry* **1993**, *97*, 3100–3110.

(44) Louie, G. V.; Brayer, G. D. High-resolution refinement of yeast iso-1-cytochrome c and comparisons with other eukaryotic cytochromes c. *Journal of Molecular Biology* **1990**, *214*, 527–555.

(45) Silkstone, G.; Jasaitis, A.; Wilson, M. T.; Vos, M. H. Ligand Dynamics in an Electron Transfer Protein. *Journal of Biological Chemistry* **2006**, *282*, 1638–1649.

(46) Bowman, S. E. J.; Bren, K. L. The chemistry and biochemistry of heme c: functional bases for covalent attachment. *Natural Product Reports* **2008**, *25*, 1118.

(47) Ye, X.; Demidov, A.; Champion, P. M. Measurements of the Photodissociation Quantum Yields of MbNO and MbO2and the Vibrational Relaxation of the Six-Coordinate Heme Species. *Journal of the American Chemical Society* **2002**, *124*, 5914–5924.

(48) Lambry, J.-C.; Vos, M. H.; Martin, J.-L. Excited State Coherent Vibrational Motion in Deoxymyoglobin. *Journal of the Chinese Chemical Society* **2000**, *47*, 765–768.

(49) Jongeward, K. A.; Magde, D.; Taube, D. J.; Traylor, T. G. Picosecond kinetics of cytochromes b5 and c. *Journal of Biological Chemistry* **1988**, *263*, 6027–6030.

(50) Mara, M. W. et al. Metalloprotein entatic control of ligand-metal bonds quantified by ultrafast x-ray spectroscopy. *Science* **2017**, *356*, 1276–1280.

(51) Wang, Q.; Wong, C. F.; Rabitz, H. Simulating Energy Flow in Biomolecules: Application to Tuna Cytochrome c. *Biophysical Journal* **1998**, *75*, 60–69.

(52) Bu, L.; Straub, J. E. Vibrational Energy Relaxation of "Tailored" Hemes in Myoglobin Following Ligand Photolysis Supports Energy Funneling Mechanism of Heme "Cooling". *The Journal of Physical Chemistry B* **2003**, *107*, 10634–10639.

(53) Fujisaki, H.; Straub, J. E. Vibrational energy relaxation in proteins. *Proceedings of the National Academy of Sciences* **2005**, *102*, 6726–6731.

(54) Agbo, J. K.; Xu, Y.; Zhang, P.; Straub, J. E.; Leitner, D. M. Vibrational energy flow across heme–cytochrome c and cytochrome c–water interfaces. *Theoretical Chemistry Accounts* **2014**, *133*, 1504.

(55) Bu, L.; Straub, J. E. Simulating Vibrational Energy Flow in Proteins: Relaxation Rate and Mechanism for Heme Cooling in Cytochrome c. *The Journal of Physical Chemistry B* **2003**, *107*, 12339–12345.

(56) Arcovito, A.; Benfatto, M.; Cianci, M.; Hasnain, S. S.; Nienhaus, K.; Nienhaus, G. U.; Savino, C.; Strange, R. W.; Vallone, B.; Della Longa, S. X-ray structure analysis of a metalloprotein with enhanced active-site resolution using in situ x-ray absorption near edge structure spectroscopy. *Proceedings of the National Academy of Sciences* **2007**, *104*, 6211–6216.

(57) Ferrante, C.; Batignani, G.; Fumero, G.; Pontecorvo, E.; Virga, A.; Montemiglio, L. C.; Cerullo, G.; Vos, M. H.; Scopigno, T. Resonant broadband stimulated Raman scattering in myoglobin. *J. Raman Spectrosc.* **2018**, *49*, 913–920.

Graphical TOC Entry